Turkish Journal of Electrical Engineering & Computer Sciences

http://journals.tubitak.gov.tr/elektrik/

Research Article

Turk J Elec Eng & Comp Sci
(2016) 24: 3492 – 3502

doi:10.3906/elk-1406-54

Reduction of torque ripple in induction motor by artificial neural multinetworks

Fatih KORKMAZ[1,*], **İsmail TOPALOĞLU**[1], **Hayati MAMUR**[1], **Murat ARI**[1], **İlhan TARIMER**[2]
[1]Department of Electrical and Electronics Engineering, ÇankırıKaratekin University, Çankırı, Turkey
[2]Department of Information Systems Engineering, Muğla SıtkıKoçman University, Muğla, Turkey

Received: 10.06.2014 • **Accepted/Published Online:** 03.05.2015 • **Final Version:** 20.06.2016

Abstract: Direct torque control is used in the high performance control of induction motors. The most frequently faced problem of it is high torque ripples. In this study, a new approach based on artificial neural multinetworks is presented to overcome the problem. Two different artificial neural networks were suggested instead of vector selection and sector determination processes in the conventional direct torque control method. The conventional and the proposed control methods were evaluated on an induction motor through an experimental set. It was observed that the speed and torque responses of the proposed method were better than those of the conventional method. The experimental results also show that the proposed method would be a good alternative to the conventional method in induction motors.

Key words: Direct torque control, induction motor, neural networks

1. Introduction

Induction motors (IMs) have vital importance in industrial applications because of their well-known advantages. In the past, IMs were generally used in constant speed applications, due to the fact that conventional speed control methods were quite expensive or inefficient. Therefore, the use of DC motors was the only option for variable speed industrial applications. However, today, the control methods of IMs have improved from simple scalar control strategies to intelligent control algorithms, thanks to the advancement of digital signal processing, power electronics, and microcontroller technologies [1].

Field-oriented control (FOC) opened a new era in the control of IMs for high performance industrial applications. Since FOC decouples the stator currents to two independent components, as a result, an IM could be controlled like DC motors. However, the success of FOC depends on many motor parameters. Therefore, the performance of FOC is directly related to accurate parameter identification. Moreover, FOC has a complex control structure on account of the necessity for coordinate transformation and the current regulators [2].

Takahashi [3] and Depenbrock [4] proposed two new control methods separately, which were called direct torque control (DTC) and the direct self-control of IMs, in the 1980s. Unlike FOC, DTC has a simple control structure. It does not require a complex coordinate transformation or any current regulators. The main idea of DTC is to choose the best vector of the voltage, which causes the flux to rotate and to produce the desired torque [5]. The core of conventional DTC (C-DTC) consists of a stator flux and a torque observer, a speed controller, an optimum switching selector, a flux, and torque hysteresis controllers. The observer estimates the actual stator flux and the torque by using the measured IM phase currents and voltages. The torque and flux references are compared with the actual values. The hysteresis controllers then produce control signals

*Correspondence: fkorkmaz@karatekin.edu.tr

[6]. Therefore, the flux and the torque can be directly controlled with the flux and the torque errors by the hysteresis controllers.

Therefore, when compared with FOC, it should be noted that DTC has not only a simple control structure, but also robustness to the parameter variations of the IM. The calculation of the stator voltage vector requires only a stator resistance from the IM parameters. Any possible variation due to the rising IM temperature in stator resistance would have a direct impact on the DTC performance. Therefore, this issue should be considered for systems operating for a long period of time. However, like every control structure, DTC has also some disadvantages such as high currents and torque ripples, difficulty to control torque and flux at very low speeds, and variable switching frequency behavior [7].

Over the last decades, DTC has become most popular due to its advantages mentioned above. Furthermore, a large number of studies to date are summarized as below:

- The investigation of different switching methods and inverter topologies [8,9]
- The implementation of artificial intelligence methods on different sections of the system [10,11]
- The investigation of different observer models [12,13].

In this paper, a new artificial neural network (ANN) approach in DTC (ANN-DTC) is presented, and two different ANN models were designed to determine the stator flux vector and optimum switching states of the inverter. Detailed information about the recommended approach is given in Section 2. The experimental studies are explained and the results of the experiments realized through torque and speed curves of an IM are given in Section 3. The experimental results, discussions, and comparisons are given in the last section.

2. Materials and methods

Over the last few decades, ANNs have gained remarkable significance because of their ability to learn, like the human brain. The potential learning abilities of ANNs extend beyond the high computation rates with the parallelism of the networks [14].

ANNs are known as computational models that are inspired by biological nervous systems. In these models, a large number of interconnected processing points (neurons) are created to work together to solve specific problems. ANNs are typically classified into three types of parameters: interconnection structure of different neuron layers, the training algorithm that is used in the training process, and activation functions that convert input data into the output of neurons. The most popular ANN employed by researchers is the multilayer feed forward ANN trained by the back propagation algorithm [15]. A recently published study has examined utilities of ANN in terms of prediction and comparison [16].

The ANN method provides computational modeling of complex and nonlinear mathematical structures. It also provides robust systems to store the data on the entire network and working ability with missing parameters in some situations. However, DTC seems simple when compared with other control methods like FOC. The DTC method also has a complex mathematical process of modeling of look-up tables, to select switching states, and to determine the stator flux section.

In this study, two different feed forward ANNs were designed to select switching states and determine the stator flux sector. Determining of the number of neurons normally requires several stages of iteration because there is no unique way to determine the optimum number of neurons. An error of estimation would be high if

the number of neurons is low. Conversely, the network would tend to memorize rather than learn [17]. In order to determine the optimum ANN structure, some off-line training results are effective in both of them.

The first model of the ANN was created to determine the flux sector. The alpha and beta components of the stator currents were operated as inputs of the flux sector determining ANN ($\mathrm{ANN}_{\lambda sector}$) as shown in Figure 1.

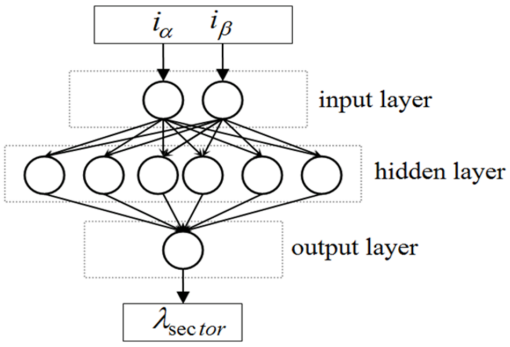

Figure 1. Presentation of stator flux sector on the $\mathrm{ANN}_{\lambda sector}$ structure.

In Figure 1, i_α, i_β, and λ_{sector} are stator currents components and flux sector data, respectively.

The $\mathrm{ANN}_{\lambda sector}$ was created in three layers and it has two neurons in the input layer, six neurons in the hidden layer, and one neuron in the output layer. The hidden layer neurons have a hyperbolic tangent sigmoid transfer function (tansig) and the output layer neuron has a linear transfer function (purelin). The input data patterns were normalized to per unit values in the input layer and they were converted to actual values (denormalization) in the output layer. The $\mathrm{ANN}_{\lambda sector}$ was trained off-line with the gradient descent (Levenberg–Marquardt) algorithm. The input and output data vectors were obtained by storage as a vector of the C-DTC stator flux sector determining block inputs and outputs. Fifty thousand data bits were used throughout the training process (35,000 data bits for training, 7500 data bits for validation, and 7500 data bits for testing). The offline training was executed for approximately 20 min with an AMD Phenom II X4 3.1 GHz processor and the best validation performance was obtained (mean squared error: 0.061978) at epoch 757 as shown in Figure 2.

The second model of the ANN was created to determine the switching states. As given in Figure 3, the torque–flux hysteresis comparator outputs and the sector of the flux were employed as inputs of the switching states selector ANN (ANN_{sw}).

In Figure 3, T_{hys}, λ_{hys}, and λ_{sector} are the torque and the flux hysteresis outputs, and the flux sector data, respectively. The MATLAB/Simulink structure of the ANN_{sw} is shown in Figure 4.

The ANN_{sw} was created in three layers and it has three neurons in the input layer, six neurons in the hidden layer, and one neuron in the output layer. The hidden layer neurons have a hyperbolic tangent sigmoid transfer function (tansig). The output layer neuron also has a linear transfer function (purelin). The ANN_{sw} was also trained off-line with the gradient descent (Levenberg–Marquardt) algorithm. The input and output data vectors were obtained by storage as a vector of the C-DTC switching state generating block inputs and outputs. Twenty-five thousand data bits were used throughout the training (15,000 data bits for training, 5000 data bits for validation, and 5000 data bits for testing). The offline training was carried out for approximately 15 min by an AMD Phenom II X4 3.1 GHz processor and the best validation performance was achieved (mean squared error: 0.076176) at epoch 543 as shown in Figure 5.

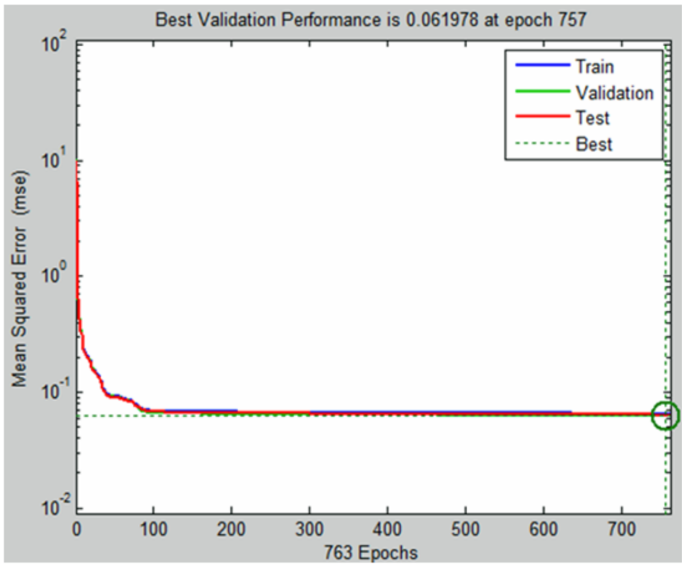

Figure 2. Training performance of the ANN $_{\lambda sector}$.

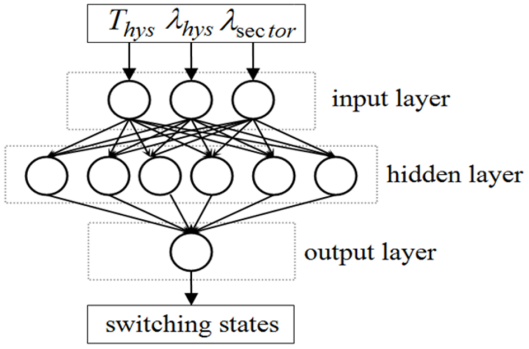

Figure 3. Presentation of switching states on the ANN $_{sw}$ structure.

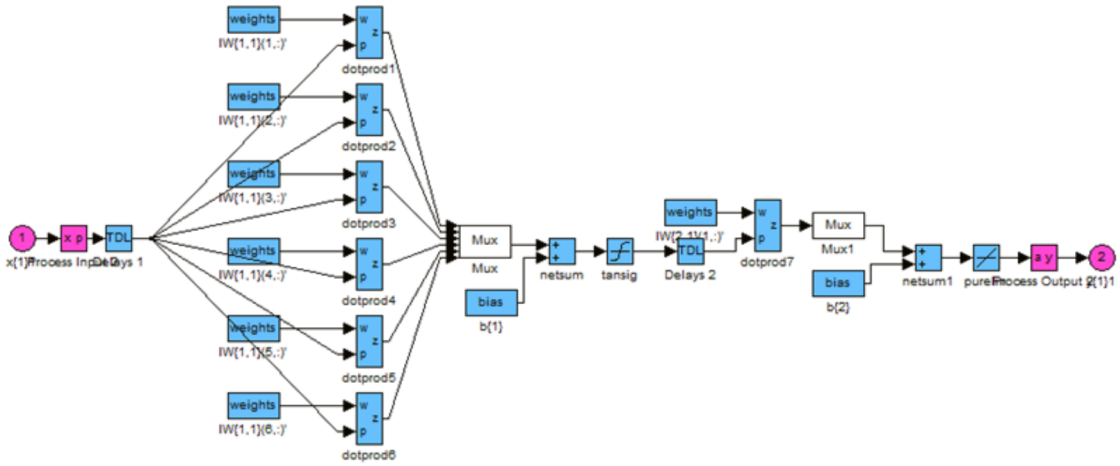

Figure 4. The ANN structure on MATLAB/Simulink.

The schematic diagram of the experimental setup is given in Figure 6. It consists of a host computer with dSPACE 1103 DSP (digital signal processor), a measurement unit, an inverter, and a motor-load group.

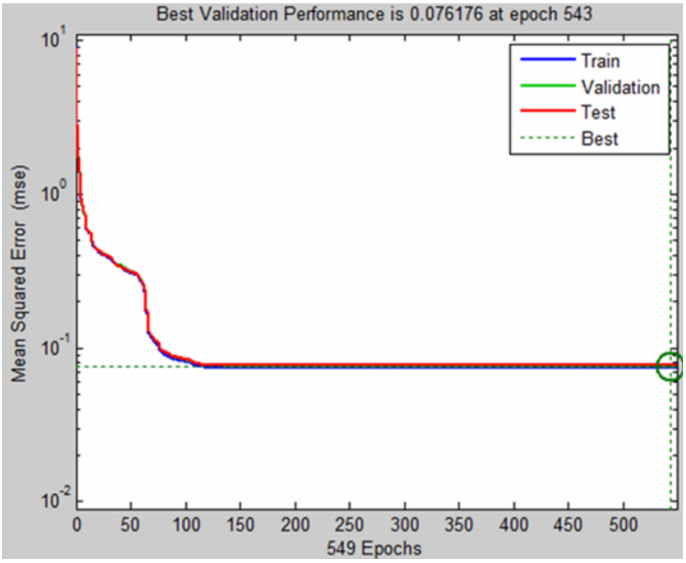

Figure 5. Training performance of the ANN $_{sw}$.

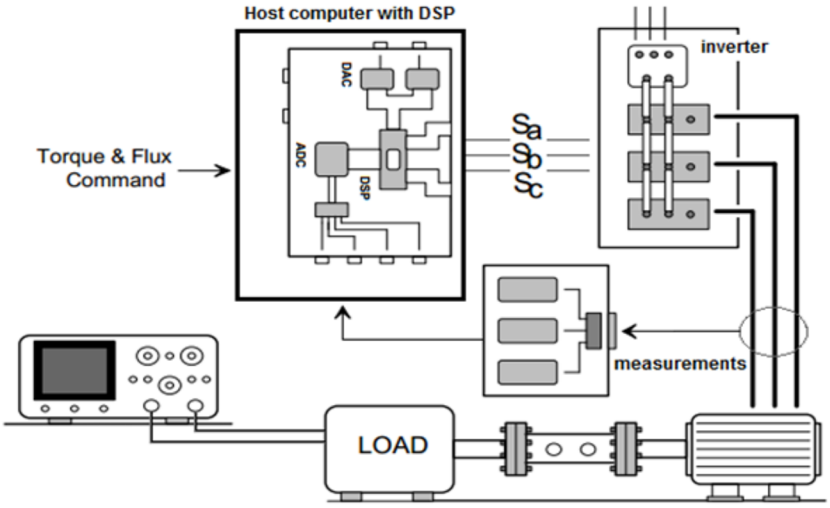

Figure 6. Schematic diagram of the experimental setup.

In the flux and torque observer model, the stator flux vector was calculated using the following equations:

$$\lambda_\alpha = \int (V_\alpha - R_s i_\alpha)\, dt \tag{1}$$

$$\lambda_\beta = \int (V_\beta - R_s i_\beta)\, dt \tag{2}$$

$$\lambda = \sqrt{\lambda_\alpha^2 + \lambda_\beta^2}, \tag{3}$$

where $\lambda_\alpha - \lambda_\beta$, $i_\alpha - i_\beta$, and $V_\alpha - V_\beta$ indicate the stator flux, the measured stator current and voltage components, respectively; α and β indicate components; and R_s depicts the stator resistance.

The electromagnetic torque of an IM is estimated using the following equation:

$$T_e = \frac{3}{2}p(\lambda_\alpha i_\beta - \lambda_\beta i_\alpha), \tag{4}$$

where p is the number of pole pairs [18].

3. Results and discussion

The dSPACE board can be integrated on MATLAB/Simulink, as one of the well-known engineering software packages. The Control Desk software is another useful feature of dSPACE that allows a graphic user interface. The user can observe the real-time responses of a control system and the parameters of the control system can also be controlled in real time.

MATLAB/Simulink Real-Time Interface (RTI) block that automatically embeds the Real-time Workshop (generated C codes) for the implementation of designed MATLAB/Simulink models on the dSPACE board provides a connection between the controller board and MATLAB/Simulink. This capability of dSPACE's allows a system designer to fully focus on the actual design process and fast determination and analysis of possible errors [19].

To perform the experimental studies, Fuji IGBT dual modules based on a voltage source inverter with gate driver circuits and an opto-isolation board were designed. A single-phase diode rectifier module with capacitive filters was used to obtain the DC voltage for the inverter. All phase voltages and currents were measured with LEM sensors (LV-25p, LA-25np). An overview of the experimental setup is given in Figure 7.

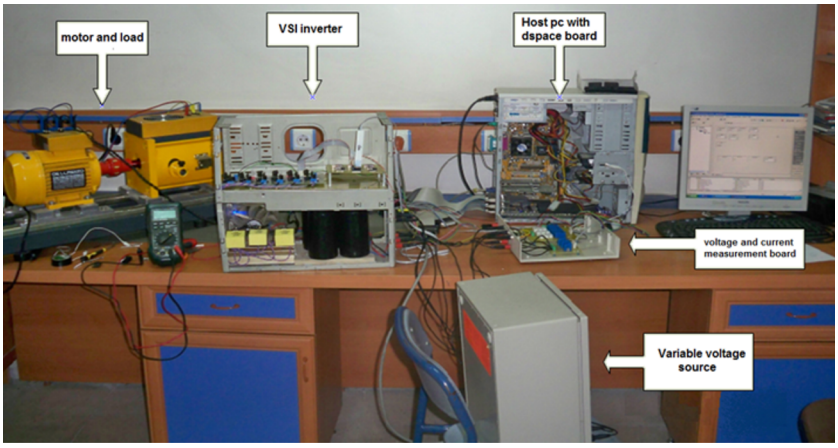

Figure 7. Overview of the test desk.

The parameters of the three-phase IM used in experimental studies are given as follows in SI units: $P =$ 1.1 kW, $U =$ 220/380 V, $I =$ 4.5/2.6 A, $cos\varphi = 0.85$, 2820 rpm, $f =$ 50 Hz, $R_s = 7.13\ \Omega$, and sampling time $= 50\ mu$ s.

Experimental studies were carried out in order to show the performance and feasibility of the proposed DTC method. The dSPACE board was programmed in the MATLAB/Simulink Real-Time-Workshop environment as shown in Figure 8.

In the C-DTC, two hysteresis controllers and stator flux section data are input parameters of a look-up table, which generates the switching states.

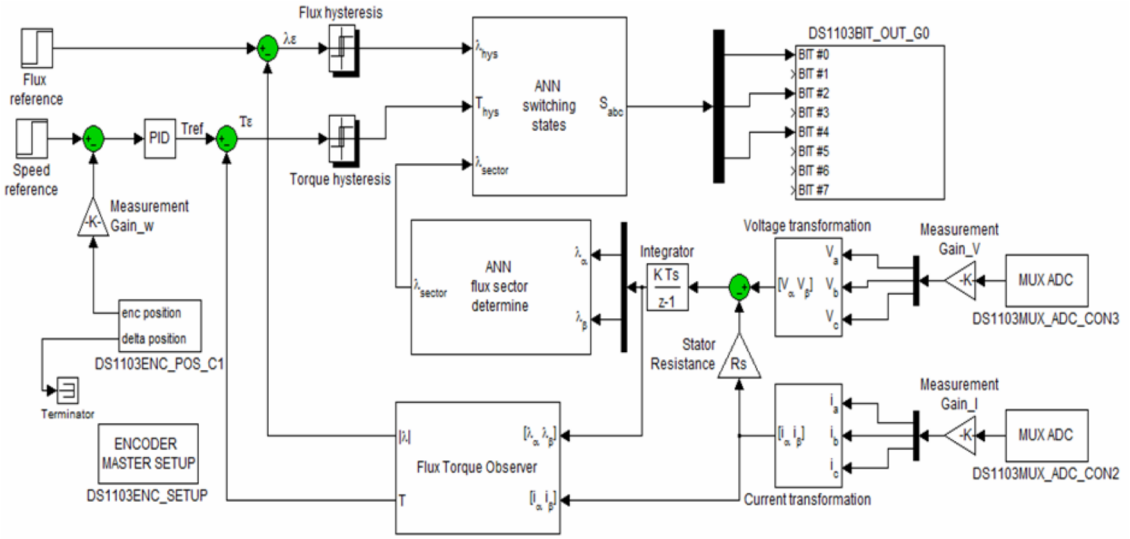

Figure 8. MATLAB/Simulink block diagram of the proposed ANN-based method.

Therefore, each of these three parameters individually affects system performance. It means that a small change in one of these parameters directly varies the output data of the switching states without considering the other two parameters. In the proposed ANN based system, the switching states and the stator flux angle were calculated by the ANNs. Thus, separately working behaviors of the parameters were eliminated. The outputs for the calculation processes were determined by an assessment of all input parameters. In other words, the input parameters of the blocks were combined with the ANN structure to determine changes in the required output values.

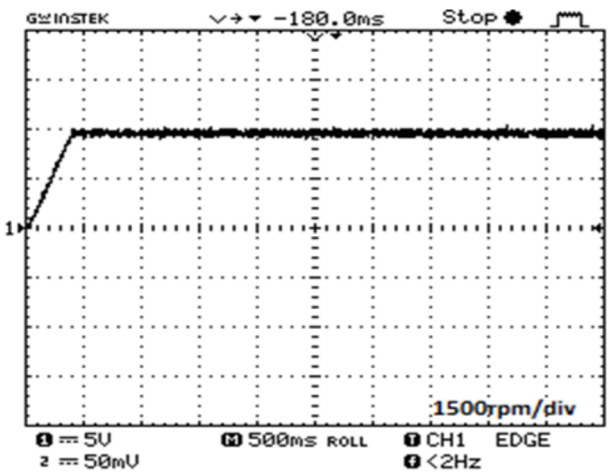

Figure 9. C-DTC controlled speed response under constant speed-variable load condition.

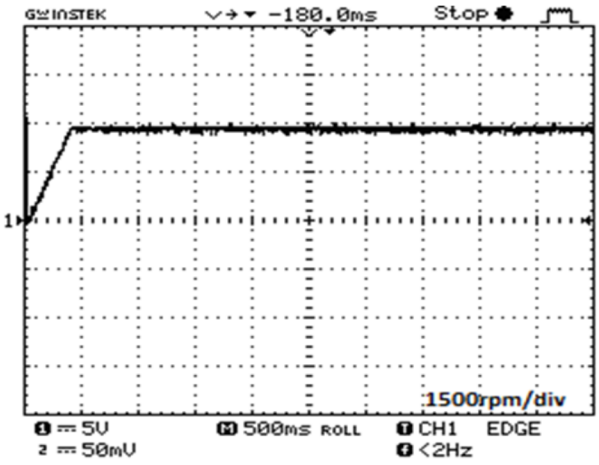

Figure 10. ANN-DTC controlled speed response under constant speed-variable load condition.

In order to evaluate a fair comparison of performances with the C-DTC and the proposed ANN-DTC, different ranges of speed and load values were applied to the IM. In the first part of the experimental tests, the IM was operated at a constant speed of 2800 rpm variable load conditions. In the tests, the IM was started at no load condition and switched to a full-load of 3 Nm at the third second and then switched to half-load of 1.5 Nm at the sixth second. The experimental results of the first part of the tests are given in Figures 9–12.

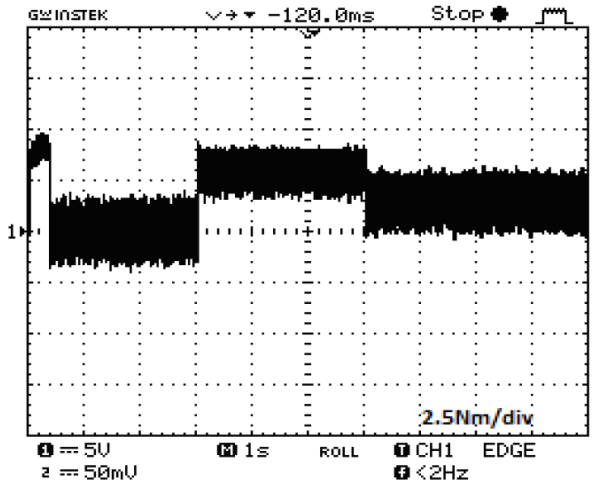

Figure 11. C-DTC controlled torque response under constant speed-variable load condition.

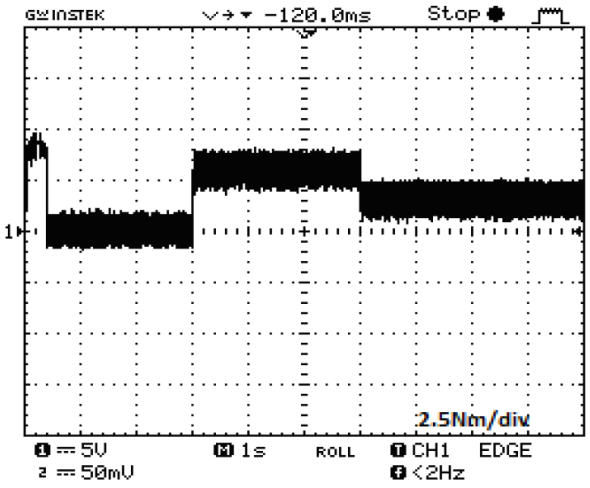

Figure 12. ANN-DTC controlled torque response under constant speed-variable load condition.

Under constant speed-variable load working conditions, Figures 9 and 10 show the responses of speed for the C-DTC and the ANN-DTC, respectively. It can be seen that similar transient responses were obtained in the IM. When the steady-state performances were compared, the same robustness was achieved against the variation of load in both of the methods.

The torque responses of the C-DTC and the ANN-DTC are given in Figures 11 and 12, respectively. By the ANN-DTC, the ripple in the torque was reduced under different load conditions.

In the second part of the tests, the IM was tested at a constant torque of 3 Nm variable speed conditions. In the tests, the IM was started at a low speed of 280 rpm, switched then to a speed of 2800 rpm at the third second, and then to the half-rate speed of 1400 Nm at the sixth second. The experimental results of the second part of the tests are given in Figures 13–16.

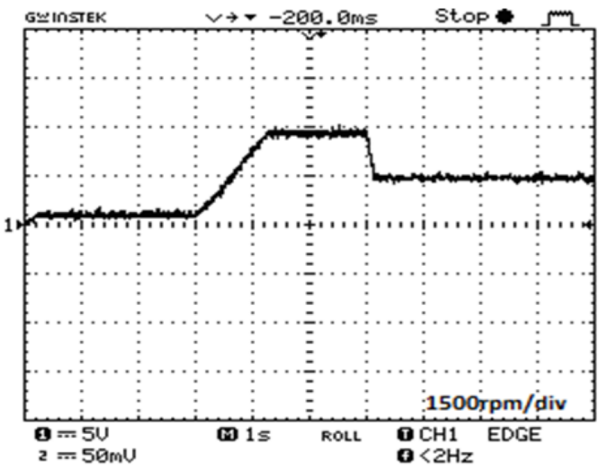

Figure 13. C-DTC controlled speed response under constant load-variable speed condition.

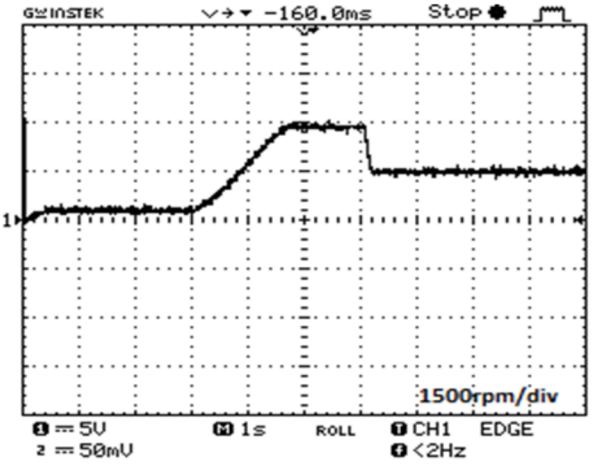

Figure 14. ANN-DTC controlled speed response under constant load-variable speed condition.

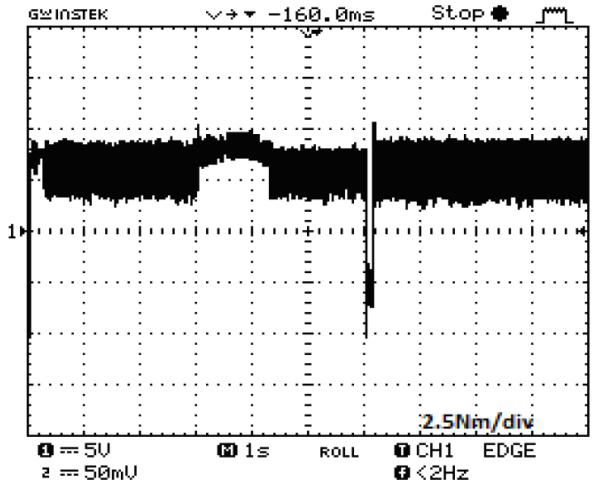

Figure 15. C-DTC controlled torque response under constant load-variable speed condition.

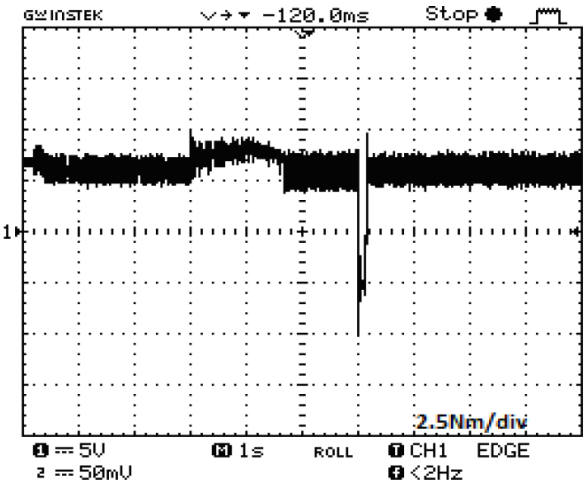

Figure 16. ANN-DTC controlled torque response under constant load-variable speed condition.

Figures 13 and 14 indicate the responses of speed for the C-DTC and the ANN-DTC in constant load-variable speed conditions, respectively. It can be inferred that both methods still have nearly the same transient responses and steady-state performances.

Figures 15 and 16 present the torque responses of the C-DTC and the ANN-DTC. Again, it should be pointed out that the ripple in torque with the ANN-DTC is less than that with the C-DTC at all speed conditions.

In order to further compare, the RMS values of torque ripples were calculated under variable load and speed conditions. In this calculation, torque values were analyzed by dividing them into two separate parts: a positive torque ripple (PTR) and a negative torque ripple (NTR). The values that are greater than the reference value were labeled as PTR and the values less than the reference value were labeled as NTR. The bandwidth of torque ripple (BTR) was calculated as given in the following equation:

$$BTR_{rms} = PTR_{rms} - NTR_{rms} \tag{5}$$

The BTR results are given in the Table. The BTR values proved that torque ripples of the IM were reduced by a rate of approximately 60%.

Table. The RMS values of bandwidth torque ripples.

IM load (Nm)		0	1.5	3
BTR_{rms} 280 rpm	C-DTC	1.18	0.58	0.52
	ANN-DTC	0.48	0.25	0.23
	Reduction rate (%)	59.32	56.89	55.76
BTR_{rms} 2800 rpm	C-DTC	1.08	0.54	0.48
	ANN-DTC	0.42	0.22	0.20
	Reduction rate (%)	61.1	59.25	58.33

During the implementation of the experimental system, different sampling times were applied to the controller. The controller board has a 1 GHz processor speed. While the C-DTC model was built in 35 mu s sampling time, the ANN-DTC model had an overloading error in this sample time. After several different time attempts, both models were built in 50 mu s sampling time. As a result of the attempts, the ANN-DTC method

required approximately 30% more computation time compared to the C-DTC. Hence, in order to implement the ANN-DTC method, designers would need to operate more powerful and quicker microcontrollers.

The experimental studies stated that the ANN-DTC method can be considered a good alternative to overcome the high torque ripples in the C-DTC method.

4. Conclusions

In this paper, ANN-based flux sector determination and a switching voltage vector selection method were proposed for DTC of IMs. The proposed method performance was compared with the C-DTC method under different speed and load conditions. The performance was also tested by experimental studies. Even though the ANN-DTC method ensured almost the same dynamic responses in a transient state, the torque ripples were remarkably reduced in the steady state. In addition, the complex mathematical structure of the C-DTC was simplified through the learning abilities of the ANNs. By the proposed method, not only did the high torque ripples remarkably decrease, but also its fast dynamic response was stabilized. Of course, the ANN structures need to have powerful and high speed microcontrollers for implementation. This situation seemed to be a drawback of the ANN systems used. The experimental results show that the proposed ANN-based DTC method can become a good alternative for DTC-controlled IMs, and it is also expected to be applicable to other motor types such as permanent magnet synchronous motors and brushless DC motors.

References

[1] Bleizgys V, Baskys A, Lipinskis T. Induction motor voltage amplitude control technique based on the motor efficiency observation. Elektron Elektrotech 2011; 3: 89-92.

[2] Lin G, Xu Z. Direct torque control of induction motor using neural network. In: Information Science and Engineering (ICISE); 26–28 December 2009; pp. 4827-4830.

[3] Takahashi I, Noguchi T. A new quick-response and high efficiency control strategy of an induction motor. IEEE T Ind Appl 1986; 5: 820-827.

[4] Depenbrock M. Direct self control of inverter-fed induction machines. IEEE T Power Electr 1988; 4: 420-429.

[5] Vas P. Sensorless Vector and Direct Torque Control. New York, NY, USA: Oxford University Press, 1998.

[6] Okumus HI, Aktas M. Adaptive hysteresis band control for constant switching frequency in DTC induction machine drives. Turk J Electr Eng & Comp Sci 2010; 18: 59-69.

[7] Zang C, Cao X. Direct torque control based on space vector modulation with adaptive neural integrator for stator flux estimation in induction motors. In: Fifth International Conference on Natural Computation (ICNC 2009); 14–16 August 2009; Tianjian, China. pp. 355-359.

[8] Casadei D, Serra G, Tani A. The use of matrix converters in direct torque control of induction machines. IEEE T Ind Electron 2001; 48: 1057-1064.

[9] Casadei D, Serra G, Tani A. Implementation of a direct torque control algorithm for induction motors based on discrete space vector modulation. IEEE T Power Electr 2000; 15: 769-777.

[10] Benaicha S, Zidani F, Said RN, Said MSN. Direct torque with fuzzy logic torque ripple reduction based stator flux vector control. In: International Conference on Computer and Electrical Engineering (ICCEE '09); 28–30 December 2009; Dubai, UAE. pp. 128-133.

[11] Sadati N, Kaboli S, Adeli H, Hajipour E, Ferdowsi M. Online optimal neuro-fuzzy flux controller for DTC based induction motor drives. In: Applied Power Electronics Conference and Exposition; 15–19 February 2009; Twenty-Fourth Annual IEEE. pp. 210-215.

[12] Tan Z, Li Y, Zeng Y. A three-level speed sensorless DTC drive of induction motor based on a full-order flux observer. In: International Conference on Power Systems Technology: 13–17 October 2002; Kunming, China: pp. 1054-1058.

[13] Ya G, Weiguo L. A new method research of fuzzy DTC based on full-order state observer for stator flux linkage. In: IEEE 2011 International Conference on Computer Science and Automation Engineering (CSAE); 10–12 June 2011. pp. 104-108.

[14] Aktas M, Okumus HI. Stator resistance estimation using ANN in DTC IM drives. Turk J Electr Eng & Comp Sci 2010; 18: 197-210.

[15] Kumar R, Gupta RA, Bhangale SV, Gothwal H. Artificial neural network based direct torque control of induction motor drives. International Conference on Information and Communication Technology in Electrical Sciences (ICTES 2007); 20–22 December 2007; IET–UK. pp. 361-367.

[16] Balli S, Tarımer I. An application of artificial neural networks for prediction and comparison with statistical methods. Elektron Elektrotech 2013; 2: 101-105.

[17] Neema DD, Patel RN, Thoke AS. Rotor flux and torque estimator for vector controlled induction drive using ANN. International Joint Conference on Neural Networks (IJCNN 2009); 14–19 June 2009; Atlanta,Georgia, USA. pp. 2215-2220.

[18] Korkmaz F, Çakır MF, Topaloğlu I, Gürbüz R. Artificial neural network based DTC driver for PMSM. International Journal of Instrumentation and Control Systems 2013; 3: 1-7.

[19] Abbou A, Nasser T, Mahmoudi H, Akherraz M, Essadki A. Induction motor controls and implementation using DSPACE. WSEAS Transactions on Systems and Control 2012; 1: 26-35.